Astronomy & Astrophysics

The isolated neutron star RBS1774 revisited[*],[**]

Revised XMM-Newton X-ray parameters and an optical counterpart from deep LBT-observations

A. D. Schwope[1], T. Erben[2], J. Kohnert[1], G. Lamer[1], M. Steinmetz[1], K. Strassmeier[1], H. Zinnecker[1], J. Bechtold[3], E. Diolaiti[4], A. Fontana[5], S. Gallozzi[5], E. Giallongo[5], R. Ragazzoni[6], C. De Santis[5], and V. Testa[5]

[1] Astrophysikalisches Institut Potsdam, An der Sternwarte 16, 14482 Potsdam, Germany
e-mail: aschwope@aip.de
[2] Argelander-Institut für Astronomie (AIfA), University of Bonn, Auf dem Hügel 71, 53121 Bonn, Germany
[3] Steward Observatory, University of Arizona, Tucson, AZ 85721, USA
[4] INAF – Osservatorio Astronomico di Bologna, via Ranzani 1, 40127 Bologna, Italy
[5] INAF – Osservatorio Astronomico di Roma, via di Frascati 33, 00040 Monteporzio, Italy
[6] INAF – Osservatorio di Padova, vicolo dell'Osservatorio 5, 35122 Padova, Italy

ABSTRACT

We report optical B-band observations with the Large Binocular Telescope (LBT) of the isolated neutron star RBS1774. The stacked image with a total exposure of $2^{\rm h}5$ reveals a candidate optical counterpart at $m_B = 26.96 \pm 0.20$ at position $\alpha(2000) = 21^{\rm h}43^{\rm m}03^{\rm s}.40$, $\delta(2000) = +06°54'17''.5$, within the joint Chandra and XMM-Newton error circles. We analyse archival XMM-Newton observations and derive revised spectral and positional parameters. The predicted optical flux from the extrapolated X-ray spectrum is likely twice as high as reported before. The measured optical flux exceeds the extrapolated X-ray spectral flux by a factor $\sim$40 (15−60 at 1σ confidence). We interpret our detection and the spectral energy distribution as further evidence of a temperature structure over the neutron star's surface and present a pure thermal model reflecting both the SED and the pulsed fraction of the light curve.

Key words. X-rays: stars – stars: neutron – stars: individual: RBS1774

1. Introduction

RBS1774 is one of the few X-ray bright, high-latitude sources found in the ROSAT all-sky survey (RASS) which remained undetected at other wavelengths despite considerable effort (Schwope et al. 2000). Based on the large X-ray to optical flux ratio implied by the non-detection at optical wavelengths, $m_R > 23$, $f_X/f_{\rm opt} > 10^3$, Zampieri et al. (2001) tentatively identified the object as a Isolated Neutron Star (INS). The ROSAT X-ray spectrum was fitted with a hot blackbody, $kT \sim 90$ eV, slightly absorbed by cold interstellar matter with a total column density of $N_{\rm H} \sim 5 \times 10^{20}$ cm^{-2}. Initial observations with XMM-Newton by Zane et al. (2005) revealed pulsations with a period of 9.437 s with a pulsed fraction of about 4%. They also revealed a spectral feature at 0.7 keV. These findings added to the accepted picture of XDINS (X-ray Dim INS) being a class of middle-aged, $\sim 10^6$ yrs, cooling NS with strong magnetic fields, $B > 10^{13}$ G (see Haberl 2007, for a recent review of the class).

Optical counterparts of four XDINS were detected with the HST, VLT, NTT, and the SUBARU telescopes in the magnitude range 25.7...28.6. In all cases the measured optical flux exceeded the extrapolated X-ray flux, typically assumed to be blackbody-like, by considerable factors. The excess flux was qualitatively explained as originating from cooler areas of the structured NS surface not detected in X-rays, see Schwope et al. (2005) or Zane & Turolla (2006) for light curve and SED modeling of XDINS. Furthermore, optical observations are important to search for parallaxes and proper motions (Motch et al. 2005, 2009) and thus constrain the likely birth place of the stars.

Despite considerable effort through multi-site, multi-band observations, RBS1774 escaped optical detection in the past (Zampieri et al. 2001; Cropper et al. 2007; Lo Curto et al. 2007). The latest compilation of optical upper limits from multi-band observations is given in Rea et al. (2007) with a most sensitive limit $m_V > 25.5$.

However, Malofeev et al. (2006) report a detection at radio wavelengths at 111.23 MHz at a brightness of 60 ± 25 mJy which, if confirmed, gives evidence for a non-thermal component in this system.

The optical non-detection gave reason to search for an optical counterpart with the newly opened Large Binocular Telescope (LBT). The object was chosen as an appropriate target in Science Demonstration Time (SDT) in October 2007.

Table 1. Summary of LBT observations of the field of RBS1774.

Date	Frames × exposure	Exposure tot	b_0
YYYYMMDD		(s)	
20071012	10×300	3000	27.68
20071014	10×300	3000	27.61
20071015	5×300	1500	27.61
20071016	$16 \times 300, 10 \times 150$	6300	–
20071018	2×150	300	27.62

All exposures were taken through a Bessel *B*-filter. The last column gives the nightly photometric zeropoint.

The observations revealed a positive detection of a likely optical counterpart.

While still analysing our LBT data, a detection of the likely optical counterpart of RBS1774 with VLT/FORS was reported by Zane et al. (2008). Hence, the current paper presents a comparison of the optical results and also presents improved X-ray spectral parameters compared to previous analyses of the same data (Zane et al. 2005; Cropper et al. 2007; Rea et al. 2007).

2. Optical observations

RBS1774 was observed with LBC-B, the blue arm of the Large Binocular Camera (Giallongo et al. 2008), during five nights in October 2007 under mostly photometric conditions. The number of frames taken together with individual exposure times are collected in Table 1. Small positional offsets between individual exposures using a variety of dither patterns ensured a continuous spatial coverage without chip gaps. The data were reduced with the GaDoDS pipeline (Erben et al. 2005), which includes basic CCD calibrations (dark, bias, flatfield correction) as well as superflat correction, astrometric and photometric calibration, and creation of a stack of all images.

A global astrometric solution was achieved using the GSC2-2, and was based on 414 (GSC) high S/N detections revealing an external astrometric accuracy $\sigma = 0''.165$ in both spatial directions.

Photometric zeropoints were determined for each night (except Oct. 16) based on observations of Stetson's standard fields. We did not re-calibrate the extinction and color terms but used the values determined by the instrument team during commissioning of the instrument[1]. The nightly zeropoints b_0 are also listed in Table 1.

The seeing varied between $0''.76$ and $1''.31$ while gathering data on RBS1774. We created two versions of a stacked image, one with the best spatial resolution using only images with a seeing better than $1''.0$ (25 images, total exposure 5700 s, seeing *FWHM* $\sim 0''.88$), and a second image with fainter limiting magnitude using all images with negligible ellipticity of stellar profiles (35 frames, total exposure 9010 s, *FWHM* seeing $0''.93$).

Source catalogues of the fully reduced *B*-band images were constructed using SExtractor (Bertin & Arnouts 1996). For a brightness determination of faint pointlike objects we use aperture magnitudes with a diameter of 8 pixels (corresponding to 1.8 arcsec). The raw magnitudes were corrected for light loss through the rather small aperture. The magnitude correction was determined by a growth curve analysis of a stellar sequence in the magnitude range 20−23 and was found to be 0.22 mag for the chosen aperture. All magnitudes quoted in this paper are in the Vega system.

_____

[1] http://lbc.oa-roma.inaf.it/commissioning/standards.html

3. XMM-Newton X-ray observations

There is one published XMM-Newton observation of RBS1774 which was performed in 2004. It was analysed and discussed by Zane et al. (2005) and Cropper et al. (2007) who give all the neccessary details of the observations. The main results of those studies were the detection of the spin frequency of 9.437 s and of a spectral feature at 0.7 keV which could be modeled as an absorption edge or an absorption line superposed on the blackbody-like continuum.

3.1. Astrometric analysis

Given the well matched large fields of view of the LBC and the XMM-Newton EPIC cameras, we attempted to improve the X-ray positional accuracy. We make use of the X-ray source list of the field as provided in the XMM-Newton Science Archive (XSA) and in the 2XMM catalogue which contains 43 sources including the target. The X-ray coordinates of RBS1774 as given in 2XMM are $\alpha(2000) = 21^h43^m03^s.22$, $\delta(2000) = +06°54'18''.0$ with an uncertainty of $\sigma = \sqrt{\sigma_{stat}^2 + \sigma_{sys}^2} = \sqrt{0.07^2 + 1.0^2} \simeq 1''.0$.

The optical and X-ray source catalogues were matched using the SAS-task eposcorr to remove remaining systematic uncertainties of the X-ray source positions due to imperfections of the spacecraft attitude. Eposcorr reported 23 X-ray/optical matches and revealed positional offsets $\Delta\alpha = 3''.0 \pm 0''.6$, $\Delta\delta = 0''.2 \pm 0''.5$, and a rotation correction of $30'' \pm 170''$. The corrected XMM-Newton position of RBS1774 is $\alpha = 325°.7643 = 21^h43^m03^s.4$, $\delta = 6°.9050 = +06°54'17''.9$ with a 1σ positional uncertainty of only $0''.7$.

The X-ray source position of RBS1774 is shifted by $2''.7$ with respect to the entry in the 2XMM source catalogue. The accuracy of the XMM-Newton X-ray position was overestimated in 2XMM; the revised position is more reliable thanks to the available optical reference positions from the wide-field LBC-observations. We note in particular that the Chandra position (we use the revised position by Zane et al. 2008) and the revised XMM-Newton positions match excellently.

3.2. Spectral analysis

X-ray spectra of the three EPIC X-ray cameras were extracted to estimate the contribution of the blackbody-like soft X-ray component of RBS1774 to the optical *B*-band. We re-processed the archival XMM-Newton data (OBSID 0201150101) with the Science Analysis Software (SAS) version 7.1. Subsequent X-ray spectral analysis was performed with XSPEC V12.3.0. The X-ray spectra were grouped in spectral bins containing at least 20 photons to allow the application of χ^2 minimisation. The spectral analysis was limited to energies between 0.2 and 1.5 keV. A fit with a pure blackbody component absorbed by cold interstellar matter (phabs * bbody in XSPEC terms) gave a poor representation of the data and revealed large systematic residuals (reduced $\chi^2 = 1.81$ for 311 degrees of freedom, see Fig. 1 for a graph of the fit and the residuals). Compared to Zane et al. (2005) and Cropper et al. (2007) we found the spectral parameters slightly changed. The amount of interstellar matter implied by the pure blackbody fit was found to be smaller in our analysis, $N_H = (1.85 \pm 0.17) \times 10^{20}$ cm^{-2} vs. $N_H = 3.65^{+0.16}_{-0.13} \times 10^{20}$ cm^{-2}, while the temperature was found to be slightly higher, $kT_{bb}^\infty = 103.5 \pm 0.8$ eV vs. $101.4^{+0.5}_{-0.6}$ eV (see Table 2 for a compilation of spectral parameters). These differences might be due

Table 2. X-ray spectral parameters of RBS1774. The errors quoted correspond to 90% confidence intervals.

No.	Model	$N_{\rm H}$ $(10^{20}\,{\rm cm}^{-2})$	$kT_{\rm bb}^{\infty}$ (eV)	$E_{\rm line}$ (eV)	$\sigma_{\rm line}$ (eV)	$\tau_{\rm line}/{\rm Norm}_{\rm line}$ (# cm^{-2} s^{-1})	χ_{ν}^2 (d.o.f.)
(1)	bbody	$1.85^{+0.17}_{-0.17}$	103.5 ± 0.8				1.81(311)
(2)	bbody*gabs	$1.84^{+0.20}_{-0.17}$	105.1 ± 0.9	$0.731^{+0.008}_{-0.013}$	27^{+16}_{-4}	$6.5^{+1.2}_{-1.0}$	1.50(308)
(3)	bbody*gabs	$3.92^{+0.75}_{-0.50}$	102.7 ± 0.8	$0.733^{+0.008}_{-0.012}$	34^{+11}_{-11}	$7.3^{+1.3}_{-1.0}$	
	+gaussian			0.31	0.03	$1.7^{+0.8}_{-0.5} \times 10^{-3}$	1.23(307)
(4)	bbody	$1.62^{+0.16}_{-0.14}$	103.9 ± 0.9				1.55(661)
(5)	bbody*gabs	$1.64^{+0.17}_{-0.15}$	105.2 ± 0.1	$0.729^{+0.004}_{-0.007}$	23^{+20}_{-19}	$4.8^{+1.7}_{-1.6}$	1.42(658)
(6)	bbody+bbody	$1.4^{+0.4}_{-0.4}$	104!				
			40!				1.05(349)

Lines (1)–(3) are combined fits to EPIC-pn and EPIC-MOS spectra in the energy interval 0.2−1.5 keV. Lines (4) and (5) represent combined fits to EPIC and RGS using the same models as in lines (1) and (2). Line (6) lists the finally accepted two-component blackbody fit to the RGS-data alone with a fixed ratio of normalization parameters.
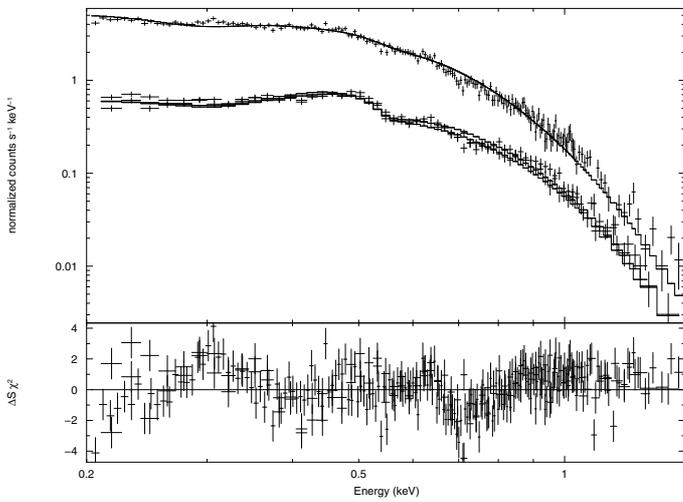
Fig. 1. Combined XMM-Newton EPIC-pn and EPIC-MOS spectra of RBS1774, fitted with a Planckian absorbed by cold interstellar matter (model (1) in Table 2).
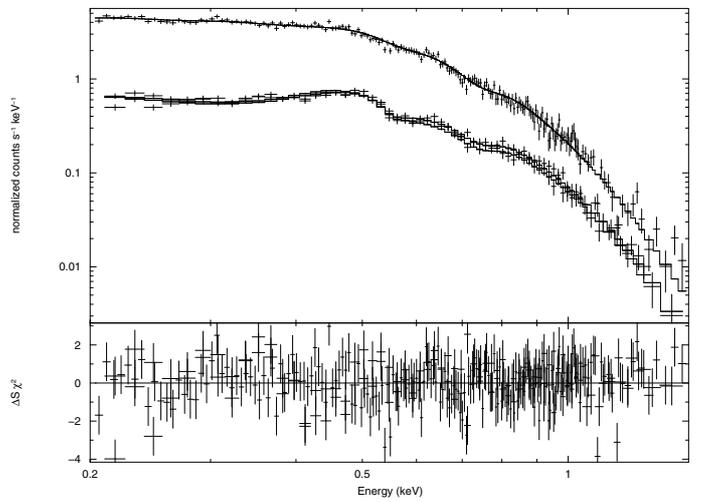
Fig. 2. Same data as in Fig. 1, fitted with a Planckian and superposed Gaussian lines absorbed by cold interstellar matter (model (3) in Table 2).

to the revised calibration of the soft X-ray spectral response of the EPIC cameras.

The feature at ∼0.7 keV first reported by Zane et al. (2005) is also evident in our spectra. Including a Gaussian absorption line at ∼0.7 keV improved the fit ($\chi_{\nu}^2 = 1.50$ for 308 degrees of freedom, see Table 2, line (2)) but still did not reveal a convincing representation of the data. The best-fit width of this line of 27 eV is narrower than the CCD resolution at this energy of ∼40 eV but still consistent at a 90% confidence level.

Large residuals around 0.31 keV in the EPIC-pn and one of the MOS cameras are evident from inspection of Fig. 1. This feature, described as an absorption line at ∼0.4 keV, was noted and discussed by Cropper et al. (2007). A feature of possible similar nature was detected in EPIC-pn spectra of the much brighter prototypical object RX J1856.4-3754 and classified as a remaining calibration problem by Haberl (2007). The same may apply to the current case of RBS1774.

However, a feature at 0.3−0.4 keV influences our determination of the amount of interstellar absorption and of the blackbody parameters. We thus included in our fit a further spectral component, a Gaussian emission line centered at 0.31 keV (model (3) in Table 2), to study the effect of modified spectral parameters on the predicted flux in the B-band. We do not claim physical reality of the emission line, but include it in the fit to explore possible

systematic uncertainties of the $T_{\rm bb}$ and $N_{\rm H}$ determination. An emission line raises $N_{\rm H}$ and hence raises the optical excess (see below) to a maximum value.

We searched for independent information for both features by extracting the spectra obtained with the RGS spectrographs onboard XMM-Newton. Both RGSs operate in the wavelength range 5−35 Å (0.33−2.5 keV), hence the feature at 0.31 keV is not fully covered. The EPIC and RGS spectra were grouped and a combined fit was performed to the EPIC- and RGS-spectra (models (4) and (5) in Table 2) forcing all parameters but the normalisations for the two groups to be the same (reduced $\chi^2 = 1.42$ for 658 d.o.f.). Then fixing the best-fitting $N_{\rm H}$ and blackbody temperature from the combined fit, the RGS-spectra were fitted separately, once with and once without the Gaussian absorption component at 0.7 keV. The reduced $\chi^2 = 1.33$ and 1.34 changed just marginally, hence the RGS spectra do not support the existence of the 0.7 keV feature. (See Fig. 3 for a blackbody fit to the RGS data.) We conclude that the nature of both features at 0.31 keV and at 0.73 keV, is uncertain; both might be real but both might be related to calibration uncertainties of the CCDs and the RGS at those very soft X-ray energies. In their analysis, Cropper et al. (2007) reach similar conclusions, they accept the feature at 0.7 keV since it could be accomodated in their RGS-fit depending on the assumed continuum, but regard the feature at
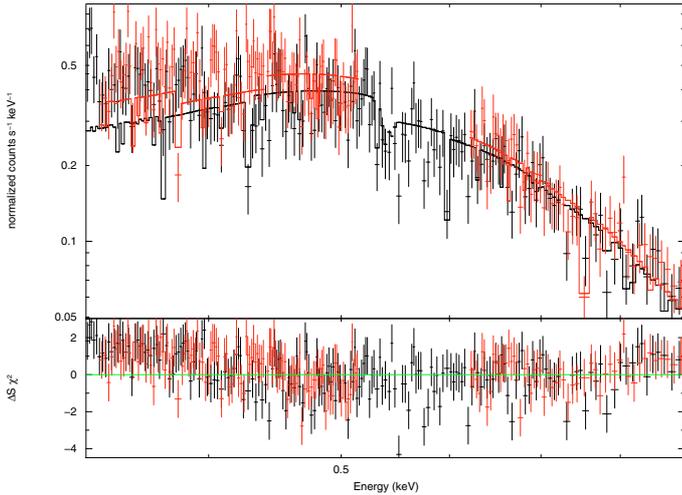
Fig. 3. RGS-spectra of RBS1774, fitted with a Planckian absorbed by cold interstellar matter (see text for details). The data gap between 0.5 and 0.6 keV is due to the dead CCD in RGS2.
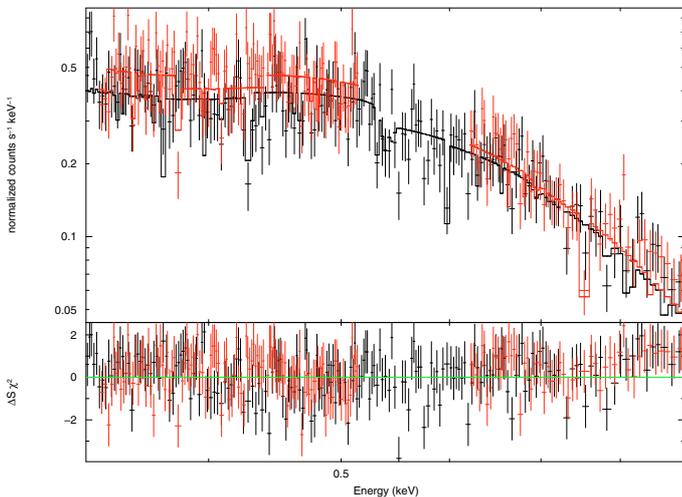

Fig. 4. RGS-spectra of RBS1774, fitted with two Planckians absorbed by cold interstellar matter. The temperatures were fixed at $k_B T_{spot} = 104$ keV and $k_B T_{star} = 40$ eV, respectively (model (6) in Table 2).

0.4 keV as unlikely. We agree that more data are necessary to prove or disprove the existence of these features.

The fit to the RGS-data alone, however, leaves large residuals. These smoothly increase towards softer X-rays, suggestive of a further low-energy radiation component. We thus attempted a fit to the RGS-data with the combination of two blackbodies, a hot component with parameters almost fixed by EPIC and a cool component responsable for the RGS soft excess. In a first attempt, all parameters were allowed to vary freely except the temperature of the hot component which was fixed at 104 keV. An excellent fit was achieved with a reduced $\chi^2 = 0.98$ for 347 d.o.f. and $kT_{cool} = 33$ eV. The absorption column density of this unconstrained fit, $N_H = 6.7 \times 10^{20}$ cm^{-2} however, exceeds the galactic value. Fixing N_H to 2.0×10^{20} cm^{-2} as implied by model (2) deteriorates the result slightly but still gives an acceptable fit, $kT_{cool} = 30$ eV at $\chi^2 = 1.03$ (348 d.o.f.). This result may be regarded as observational evidence for the presence of a cooler radiation component in RBS1774.

The amount of interstellar absorption, N_H, was typically found to be lower than the total galactic column density,
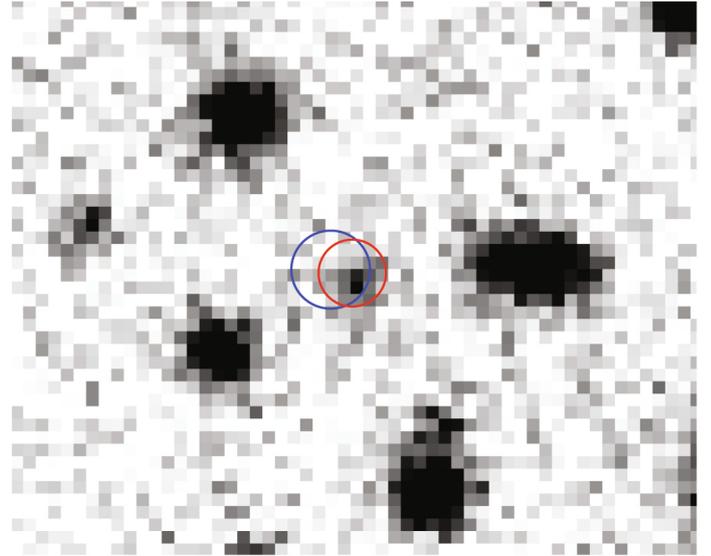
Fig. 5. LBT B-band image of the region of RBS1774 with north at the top and east to the left (pixelsize 0.″225). Error circles illustrate the corrected Chandra (red) and XMM-Newton (blue) X-ray positions.

$N_{H,gal} = 4.83 \times 10^{20}$ cm^{-2} in the direction of RBS1774 ($l^{II} = 62.66°$, $b^{II} = -33.1°$). Only the inclusion of the additional absorption at 0.31 keV raised N_H close to its galactic value. The unabsorbed flux in the B-band of the first three models listed in Table 2 lies between $F_E = 2.8 \times 10^{-6}$ erg cm^{-2} s^{-1} keV^{-1} and 4.3×10^{-6} erg cm^{-2} s^{-1} keV^{-1} at a 90% confidence level (apparent magnitude 30.9...30.4). Both the minimum and the maximum value lie above the extrapolation of Zane's fit into the optical (Zane et al. 2005; Rea et al. 2007), $F_E = 2.2 \times 10^{-6}$ erg cm^{-2} s^{-1} keV^{-1} ($m_B = 31.2$), the maximum flux estimated by us is more than a factor of 2 higher than the old value. This is only partly due to the additional Gaussian, and part of this effect is possibly due to an improved calibration of the X-ray cameras.

4. An optical counterpart to RBS1774 from LBC-imaging

Figure 5 shows an expansion of the large LBT-image zoomed and centered on the X-ray position of RBS1774. The revised Chandra (Zane et al. 2008) and the revised XMM-Newton X-ray error circles are also shown. We confirm the detection of an optical counterpart to the X-ray source at a position of $\alpha(2000) = 21^h43^m03^s.40$, $\delta(2000) = +06°54'17''.5$. It lies in the joint region of the error circles from both Chandra and XMM-Newton. Positional offsets with respect to the X-ray positions are 0.″21 and 0.″55, respectively. We cannot compare our optical position with that of Zane et al. (2008), since no absolute position is given there, just a positional offset of 0.″2 with respect to the revised Chandra position, the same as ours. Their Figs. 1 and our 5 display marginal apparent differences between the counterpart positions and the Chandra error circles and we conclude that the optical source positions are the same within the given errors.

The object detected by us has an apparent magnitude of $m_B = 26.^m96 \pm 0.^m15$ (1σ statistical error). The color of the object is not known, and a color correction with a blue, blackbody-like object would change the apparent magnitude by 0.05 mag, which we include in the error budget. Hence, our final photometric error is 0.2 mag. Our measurement reveals a counterpart
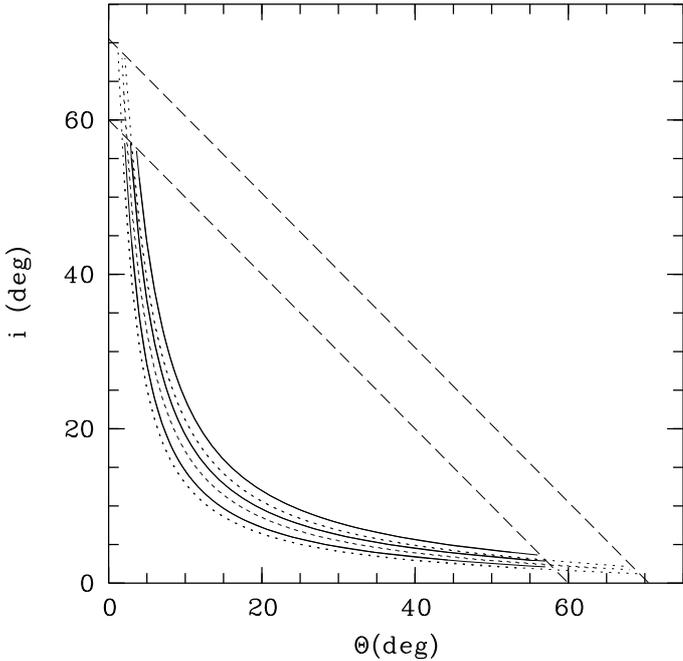
Fig. 6. Spot locations in the $i - \theta$ plane asuming an emission radius $R = 3\,r_S$ (sold line) and $4\,r_S$ (dotted lines) and pulsed fractions of 3–5%, respectively. The dashed lines mark the limit of class I light curves for the chosen compactness.

Fig. 7. Spectral energy distribution of RBS1774. Shown are the unfolded X-ray spectrum in black, the absorption-corrected fit to the X-ray spectrum in blue (model 2 in Table 2), the measured B-band fluxes corrected for interstellar absorption and an SED model involving a hot 104 eV spot on a cool 40 eV star (magenta, model (6) in Table 2). The absorbed and absorption-corrected contribution of the cool stellar surface is shown red.
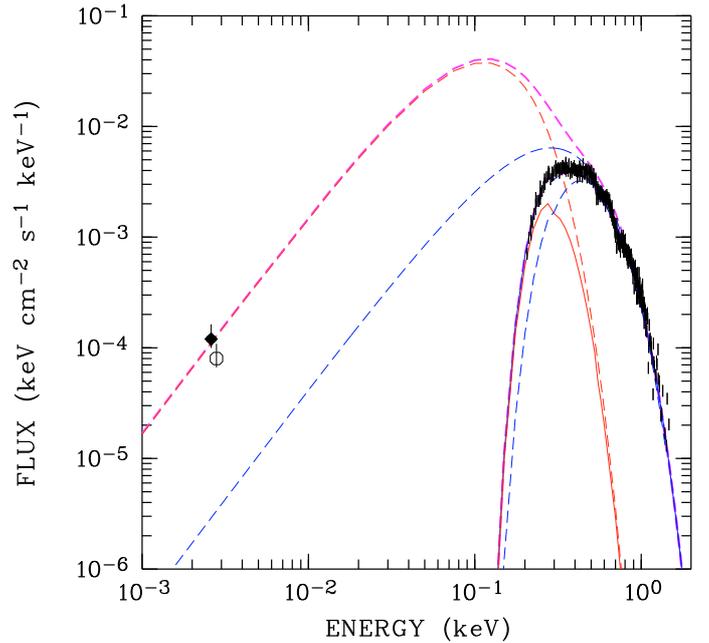
that is brighter by 0.4 mag compared to the detection by Zane et al. (2008). Both measurements have an uncertainty of 0.2 mag. Hence, the brightness difference might be real. If confirmed, the optical counterpart of RBS1774 would be the first among its class displaying brightness variations.

5. Discussion

The amount of interstellar absorption as determined from the X-ray spectral fits is in the range $N_H = (1.8-3.6) \times 10^{20}$ cm^{-2}. Assuming galactic dust with $R = 3.1$ the absorption in the B-band is $\Delta m_B = 0\overset{m}{.}13-0\overset{m}{.}27$, which we use to correct the magnitude found by us. Hence, the optical excess over the extrapolated flux from the X-ray spectral fits is in the range between 15 and 60 (dependent on the assumed brightness, the amount of interstellar absorption and the assumed X-ray spectral parameters), larger than for any other objects of its class. Taking the parameters from the X-ray spectral model (2) and $m_B = 26.96$, $\Delta m_B = 0.13$ as face values, the optical excess is 40.

There are some lines of evidence for a non-homogeneous temperature distribution over the star's surface, (a) a pulsed X-ray light curve; (b) an optical excess; and (c) the likely presence of a second, cooler, component in the RGS-spectrum. We first discuss the simplest model of antipodal circular polar caps and a cooler stellar surface.

Light bending and light curves of antipolar caps have been studied by Pechenick et al. (1983) and Beloborodov (2002). Beloborodov (2002) classified types of light curves depending on the viewing geometry. According to this classification the light curve of RBS1774 is of class I, with only one hot spot being persistently in view and the second never being visible. The pulsed fraction gives an implicit equation between i and θ, the inclination of the rotation axis and the latitude of the spot. The solution of this equation depends on the assumed compactness of the star, i.e. the radius of emission in units of the Schwarzschild

radius r_S. Solutions are shown in Fig. 6 for $R_{em} = 3\,r_S$ and $4\,r_S$, respectively and pulsed fractions in the range 3–5%, respectively. The X-ray light curve has a pulsed fraction of about 4% (Zane et al. 2005). The allowed ranges in i and θ go up to surprisingly large angles (57° for $R_{em}/r_S = 3$, 68° for $R_{em}/r_S = 4$), thus alleviating the conclusion of Zane et al. (2008) that both angles are smaller than 20°. However, if one of the two angles takes its maximum value, the corresponding angle has to become very small. Such an extreme geometry seems unlikely and a geometry described by Zane et al. (2008) is more preferred but it seems still to be consistent with the data.

The observed spectral energy distribution of RBS1774 from the optical to the X-ray range is displayed in Fig. 7. Following Schwope et al. (2005) we synthesise the observed spectral energy distribution (SED) with the combination of a hot spot, $k_B T_{spot}$, and a cool stellar surface, $k_B T_{star}$.

An indication of the possible surface temperature was derived above, $k_B T_{star} \simeq 40$ eV, which we assume in the following without loss of generality. A final fit to the RGS spectrum was performed with fixed temperatures, $k_B T_{spot} = 104$ eV and $k_B T_{star} = 40$ eV, respectively, and a fixed ratio of the normalization parameters of the two blackbody components. A fixed ratio of the normalizations is required to reflect the observed optical excess. At the same time, it fixes the relative sizes of the spot and star radius (spot opening angle) for the chosen set of temperatures. Free fit parameters were the column density and the normalization parameter of the hot component. The latter quantity in combination with the fixed ratio of normalization parameters encodes $R_{ns,\infty}/d$. The fit was successful (reduced $\chi^2_\nu = 1.05$ for 348 d.o.f) and yielded a column density well below the galactic value, $N_H = (1.4 \pm 0.4) \times 10^{20}$ cm^{-2}. The fit and the residuals are shown in Fig. 4 (model parameters also listed in Table 2, line (6)).

The same model applied to the three EPIC spectra does not improve the fit compared to model (2, single blackbody) and we conclude that either the EPIC spectrum is intrinsically more complex or that remaining calibration uncertainties prevent final conclusions.

Given the simplicity of the model, the model SED shown in Fig. 7 is merely illustrative. It assumes a compactness $R_{ns}/r_s = 4$, $R_\infty = 13.8$ km, a distance of 250 pc, and a spot opening angle of 6.5°. The derived spot opening angle corresponds to a radius of 1.6 km at 250 pc which compares well with the estimate of Cropper et al. (2007) who derive $r_X = 2$ km at an assumed distance of 300 pc.

The chosen model successfully reflects the observed SED, but a two-temperature atmosphere appears to be artificial. Such a temperature distribution would likely require outside heating, either from a magnetosphere or from accretion. Whether the most recent calculations of neutron star crusts (Geppert et al. 2006) could mimic such a temperature distribution needs to be tested. Using our parameterization of the older models by Geppert et al. (2004) we could not find a model reflecting the SED with an optical excess of a factor of 40. However, as we have shown, the optical excess is uncertain and needs a more precise determination with better data.

The distance of 250 pc should be regarded as lower limit to the star. A smoother and thus more realistic temperature distribution will yield a larger distance.

Whether the currently available data on RBS1774 are consistent with just thermal radiation needs further investigation. Zane et al. (2008) discuss alternative possibilities for the observed optical excess in RBS1774, powered either by magnetospheric radiation or by magnetic field decay, both leading to a non-thermal radiation component. These alternative possibilities can be distinguished rather straightforwardly by further multi-band deep imaging.

References

Beloborodov, A. M. 2002, ApJ, 566, L85
Bertin, E., & Arnouts, S. 1996, A&AS, 117, 393
Cropper, M., Zane, S., Turolla, R., et al. 2007, Ap&SS, 308, 161
Erben, T., Schirmer, M., Dietrich, J. P., et al. 2005, Astron. Nachr., 326, 432
Geppert, U., Küker, M., & Page, D. 2004, A&A, 426, 267
Geppert, U., Küker, M., & Page, D. 2006, A&A, 457, 937
Giallongo, E., Ragazzoni, R., Grazian, A., et al. 2008, A&A, 482, 349
Haberl, F. 2007, Ap&SS, 308, 181
Lo Curto, G., Mignani, R. P., Perna, R., & Israel, G. L. 2007, A&A, 473, 539
Malofeev, V. M., Malov, O. I., Teplykh, D. A., et al. 2006, The Astronomer's Telegram, 798, 1
Motch, C., Sekiguchi, K., Haberl, F., et al. 2005, A&A, 429, 257
Motch, C., Pires, A. M., Haberl, F., Schwope, A., & Zavlin, V. E. 2009, A&A, 497, 423
Pechenick, K. R., Ftaclas, C., & Cohen, J. M. 1983, ApJ, 274, 846
Rea, N., Torres, M. A. P., Jonker, P. G., et al. 2007, MNRAS, 379, 1484
Schwope, A., Hasinger, G., Lehmann, I., et al. 2000, Astron. Nachr., 321, 1
Schwope, A. D., Hambaryan, V., Haberl, F., & Motch, C. 2005, A&A, 441, 597
Zampieri, L., Campana, S., Turolla, R., et al. 2001, A&A, 378, L5
Zane, S., & Turolla, R. 2006, MNRAS, 366, 727
Zane, S., Cropper, M., Turolla, R., et al. 2005, ApJ, 627, 397
Zane, S., Mignani, R. P., Turolla, R., et al. 2008, ApJ, 682, 487